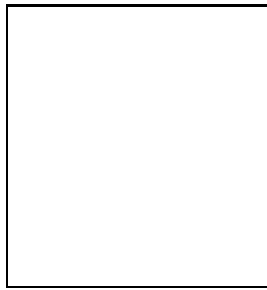


Dibosons at the Tevatron

Elliot Lipeles

CERN, CH-1211 Genève 23, Switzerland



Recent developments in the study diboson production at the Tevatron are reviewed. These include indications at the 2.6σ level for a radiation amplitude zero in the $W\gamma$ process at $D\bar{O}$ and a 4.4σ signal for ZZ production in hadron collisions from CDF.

1 Introduction

The process of the simultaneous production of two electroweak bosons is one of the few tree-level processes that is sensitive to the couplings between gauge bosons. These couplings are a direct consequence of the non-abelian group structure of the standard model (SM). At the Tevatron, a broad program of measuring cross-sections and kinematic distributions is aimed testing whether these processes are consistent with the SM predictions and searching for evidence of non-standard model contributions. The WW and ZZ final states are also of interest as potential Higgs search channels.

The leading-order Feynman diagrams for diboson production are shown in Figure 1. The t -channel shown in Figure 4(a) is effectively two copies of single boson production and involves only the fermion to boson couplings. The s -channel shown in Figure 4(b) involves the triple gauge couplings. In the standard model, only the $WW\gamma$ and WWZ vertices are non-zero; the $Z\gamma\gamma$, $ZZ\gamma$, and ZZZ vertices do not exist.

The CDF and $D\bar{O}$ have studied the $W\gamma$, $Z\gamma$, WZ , and ZZ final states in 1-2 fb^{-1} of $p\bar{p}$ collisions at 1.96 TeV produced by the Tevatron. A summary of the predicted and observed cross-sections is shown in Figure 1(c). Shown for comparison are the single boson production cross-sections which present a significant experimental challenge because they are three to four orders of magnitude larger than the diboson cross-sections.

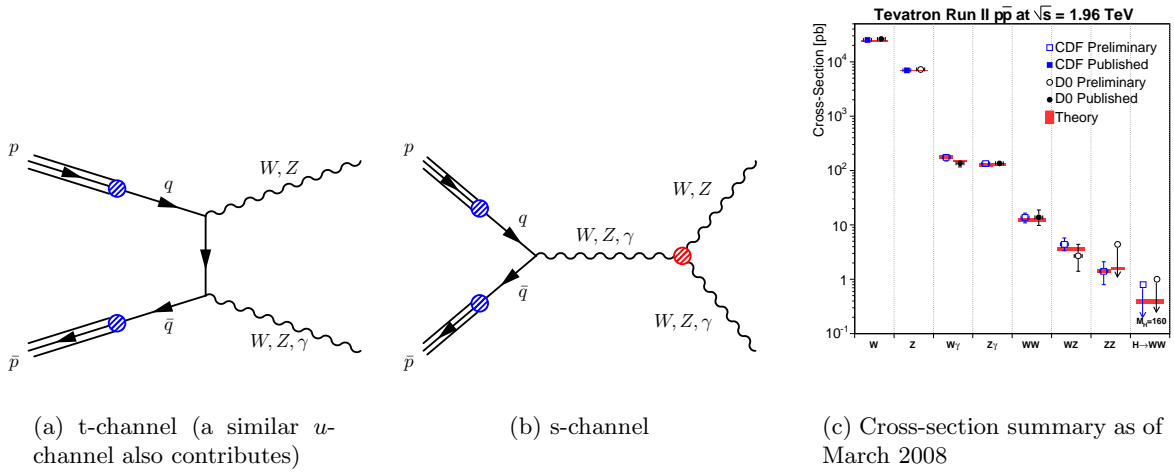


Figure 1: Feynman diagrams contributing to diboson production at leading order and a summary of diboson cross-section measurements.

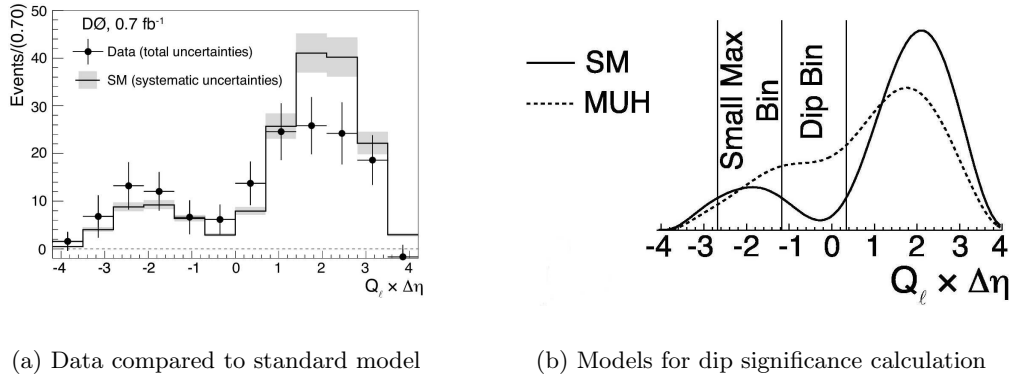


Figure 2: The $Q_l \times (\eta_\gamma - \eta_l)$ distribution for $D0 W\gamma$ events.

2 Radiation Amplitude Zero

In the $W\gamma$ process, the two Feynman diagrams shown in Figure 1 interfere destructively. This interference is complete when the angle of the W^\pm relative to the incoming quark in the $W\gamma$ rest-frame is $\pm\frac{1}{3}$ causing the leading-order differential cross-section to completely disappear in what is known as the radiation amplitude zero (RAZ). Although long predicted¹, it is difficult to observe because the missing neutrino information when W is reconstructed in the $l\nu$ final state. There is however an approximate zero in the quantity $Q_l \times (\eta_\gamma - \eta_l)$ where Q_l is the lepton charge, and η_γ and η_l are the pseudo-rapidities of the photon and lepton respectively². The observation of the zero would be a demonstration of the presence of the $WW\gamma$ vertex contribution to the $W\gamma$ process.

Using 0.7 fb^{-1} of $p\bar{p}$ collisions, $D0$ has reconstructed a sample of $W\gamma \rightarrow l\nu\gamma$ events where l is either e or μ ¹. The $Q_l \times (\eta_\gamma - \eta_l)$ distribution of these events, after subtracting the estimated background, it shown in Figure 2(a). In order to quantify the significance of the dip, a minimal unimodal hypothesis (MUH) is constructed by choosing a set of $WW\gamma$ couplings such that there is no dip in the distribution (shown in Figure 2(b)). They then find that it is ruled out at the 2.6σ level.

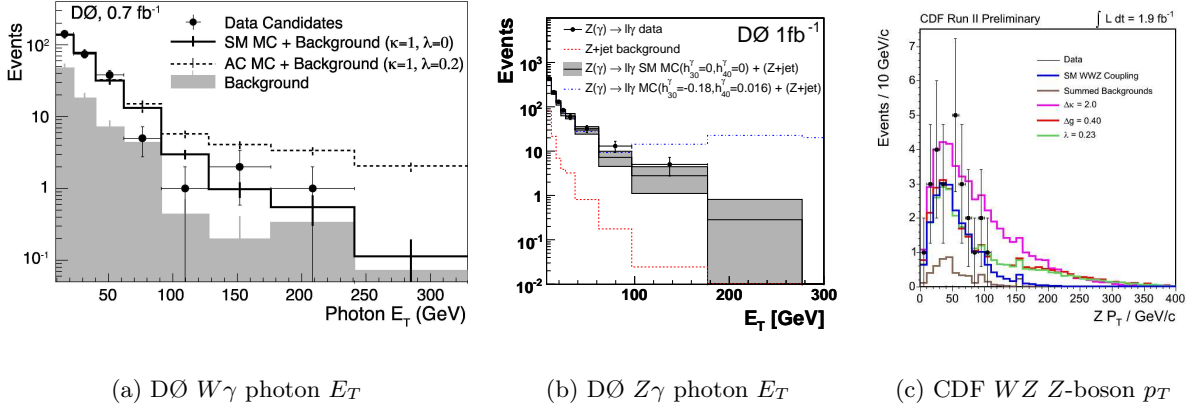


Figure 3: Distributions used to set limit on anomalous triple gauge couplings

3 Triple Gauge Couplings

Deviations of the boson to boson couplings from the SM are referred to as anomalous triple gauge couplings (aTGCs) and are parameterized by adding terms to the SM Lagrangian; for example for the $WW\gamma$ vertex:

$$\mathcal{L}_{aTGC}/ig_{WW\gamma} = \Delta\kappa_\gamma W_\mu^* W_\nu F^{\mu\nu} + \frac{\lambda_\gamma}{M_W^2} W_{\rho\mu}^* W_\nu^\mu F^{\nu\rho} \quad (1)$$

where the form-factors λ_γ and $\Delta\kappa_\gamma$ are zero in the SM. In addition to differences in the integrated cross-sections, anomalous TGCs typically give rise to significant enhancements at large diboson invariant mass \hat{s} . In fact aTGCs can cause unitarity violations at large \hat{s} , so the form-factors must be constructed so as to turn off as \hat{s} gets large; e.g. $\lambda_\gamma(\hat{s}) = \lambda_\gamma/(1 + (\hat{s}/\Lambda)^2)^2$ where Λ is typically 1.5 to 2.0 TeV. This also means that these form-factors are intrinsically energy dependent and Tevatron limits should be considered as complimentary to the LEP limits which are at $\hat{s} \approx 2M_W$. CDF and DØ have recently updated limits on aTGCs using the $E_T \gamma$ distributions for $W\gamma$ (DØ)[?] and $Z\gamma$ (CDF and DØ), the Z boson p_T for WZ (CDF and DØ), and the cross-section alone for ZZ (DØ)⁴. Sample distributions used in the limit setting are shown in Figure 3.

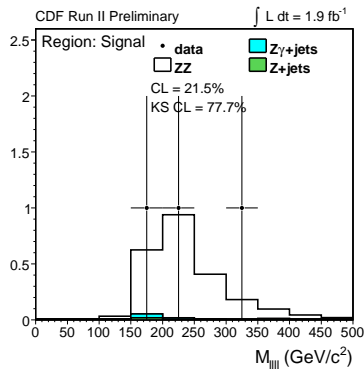
4 Evidence of ZZ Production

The ZZ final state is the only SM diboson state not yet conclusively observed in hadron collisions (not including those involving the Higgs) and is unique in providing access to the ZZZ coupling. DØ has searched in the four charged-lepton $llll$ channel⁴ finding 1 candidate event in 1.0 fb^{-1} of data with an expected signal yield of 1.71 ± 0.15 events and background of 0.13 ± 0.03 events. Based on this search an upper limit of $\sigma(ZZ) < 4.4 \text{ pb}$ is set to be compared to an NLO prediction of 1.6 pb.

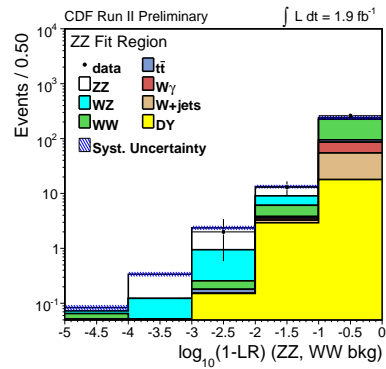
CDF finds a 4.4σ signal for ZZ production⁵ using 1.9 fb^{-1} of data by combining the $llll$ (4.2σ) and $ll\nu\nu$ (1.2σ) channels. The $llll$ channel is subdivided into two categories based on whether the candidate contains an electron that occurs outside the acceptance of the tracking system and therefore has a significantly large background rate. Three $llll$ candidate events are found with the predicted signal and background yields shown in Table 1. In the $ll\nu\nu$ channel, a matrix-element (ME) based probability calculation is used to separate the ZZ signal from the much larger WW background. The likelihood ratio from the ME calculation is shown in Figure

Table 1: Expected and observed number of $ZZ \rightarrow llll$ candidate events. The first uncertainty is statistical and the second one is systematic.

Category	Candidates without a trackless electron	Candidates with a trackless electron
ZZ	$1.990 \pm 0.013 \pm 0.210$	$0.278 \pm 0.005 \pm 0.029$
Z +jets	$0.014^{+0.010}_{-0.007} \pm 0.003$	$0.082^{+0.089}_{-0.060} \pm 0.016$
Total	$2.004^{+0.016}_{-0.015} \pm 0.210$	$0.360^{+0.089}_{-0.060} \pm 0.033$
Observed	2	1



(a) Four lepton invariant mass distribution



(b) Matrix-element discriminator for $ll\nu\nu$

Figure 4: Distributions from the CDF ZZ search

4 along with the four lepton invariant mass distribution from the $llll$ channel. The corresponding measured cross-section $\sigma(p\bar{p} \rightarrow ZZ) = 1.4^{+0.7}_{-0.6}$ (stat.+syst.) pb is consistent with the standard model expectation.

5 Summary

The increased luminosity at the Tevatron has allowed for substantial progress in diboson physics and marks entry into a new sensitivity regime where electroweak bosons are now being pair produced in significant numbers. Recent accomplishments include 2.6σ signal for the RAZ in $W\gamma$, a 4.4σ signal for ZZ production, and a number of anomalous couplings limits that continue to improve.

References

1. K. O. Mikaelian, M. A. Samuel and D. Sahdev, *Phys. Rev. Lett.* **43**, 746 (1979).
2. U. Baur, S. Errede and G. L. Landsberg, *Phys. Rev. D* **50**, 1917 (1994).
3. V. M. Abazov *et al.* [DØ Collaboration], arXiv:0803.0030 [hep-ex].
4. V. M. Abazov *et al.* [DØ Collaboration], *Phys. Rev. Lett.* **100**, 131801 (2008).
5. T. Aaltonen *et al.* [CDF Collaboration], arXiv:0801.4806 [hep-ex].